Available online at www.sciencedirect.com
ScienceDirect
Journal of Power Sources 176 (2008) 112–117
JOURNAL OF POWER SOURCES
www.elsevier.com/locate/jpowsour

Short communication

Kinetic characterization of a Pt–Ni/C catalyst with a phosphoric acid doped PBI membrane in a proton exchange membrane fuel cell

K.C. Neyerlin *, Amarveer Singh, Deryn Chu

U.S. Army Research Laboratory, 2800 Powder Mill Road, Adelphi, MD 20783, United States

Received 20 August 2007; received in revised form 10 October 2007; accepted 11 October 2007
Available online 18 October 2007

Abstract

The performance of a phosphoric acid doped polybenzimidazole (PBI) membrane, with Pt and Pt–Ni/C catalysts on the anode and cathode, respectively, was experimentally determined at 160 °C using neat H_2 and O_2. The resulting current voltage relation was then compared to a performance curve calculated from previously established values for the exchange current density and activation energy of the oxygen reduction reaction (ORR) on Pt–Ni/C. An overall voltage loss >200 mV, regardless of current density, was observed for the MEA relative to the predicted performance, implying about two orders of magnitude decrease in the exchange current density for the ORR. The reduction in exchange current density was attributed to anion ($H_2PO_4^-$) adsorption.
Published by Elsevier B.V.

Keywords: Fuel cells; Oxygen reduction; Anion adsorption; Platinum–Nickel; PBI; High temperature

1. Introduction

Proton exchange membrane fuel cells (PEMFC) that can operate simultaneously at high temperature (>120 °C) and low relative humidity (RH) are desired to improve water management and facilitate the removal of waste heat [1,2]. Moreover, the high temperatures (>120 °C) serve to both limits the adsorption of CO on Pt [3–5], a poison that lowers the kinetics of hydrogen oxidation reaction (HOR) and ORR [6], as well as increase the kinetics of the ORR due to the substantial activation energy of the reaction. For example, an increase in operating temperature from 80 to 160 °C increases the rate of the ORR on Pt/C by two orders of magnitude [7]. Nevertheless, high temperature proton conducting materials would have to provide sufficient conductivity (on the order of 0.1 S cm^{-1}) at low to zero relative humidity, since maintaining high levels of humidification makes for a more complex system at such high temperatures.

Investigations into high temperature proton exchange membrane materials have increased in recent years; with phosphoric acid doped PBI (polybenzimidazole)-based materials showing promise [8,9] (i.e. reasonable conductivities with no additional external humidification). However, recently, Lobato et al. attributed increases in charge transfer resistance for the ORR to electrochemical surface area reduction caused by the phosphoric acid electrolyte [10]. Correspondingly, phosphoric acid poisoning of the cathode catalyst has been proposed as the primary reason behind large amounts of catalyst required to elicit reasonable cell performance [11]. If this is indeed true, depending on the extent to which the acid alters the performance of the catalyst, the benefits of high temperature operation may be completely erased.

This study serves to establish a kinetic baseline for the performance of a phosphoric acid doped PBI membrane having a Pt/C anode and a Pt–Ni/C cathode. By comparing the experimental results obtained here with performance predicted from previous studies of the ORR on Pt–Ni/C catalysts, we will be able to isolate the extent to which the rate of the ORR is altered.

2. Theoretical background

In the absence of mass transport and anode voltage loss considerations (i.e. $\eta_{HOR} \approx 0$, see Section 4 and Ref. [12]) [12], the anticipated performance of a PEMFC ($E_{iR\text{-free}}$) relies primarily upon the reversible cell voltage (E_{rev}) and the voltage loss due to

* Corresponding author. Present address: University of Houston, Department of Chemical and Biological Engineering, 4800 Calhoun Road, Engineering Building 1, Houston, TX 77004, United States. Tel.: +1 713 743 5620; fax: +1 713 743 4323.
E-mail address: kcneyerlin@uh.edu (K.C. Neyerlin).

0378-7753/$ – see front matter. Published by Elsevier B.V.
doi:10.1016/j.jpowsour.2007.10.030

the kinetics of the oxygen reduction reaction (η_{ORR}) (Eq. (1)):

$$E_{iR\text{-free}} = E_{rev} - \eta_{ORR} \quad (1)$$

The reversible cell potential at ambient pressures of H_2 and O_2 as a function of temperature and relative humidity can be given by Eq. (2) [13]:

$$E_{rev} = 1.23 - 0.9 \times 10^{-3}(T - 298) - \frac{RT}{2F} \ln\left(\frac{RH}{100}\right) \quad (2)$$

where T is the operating temperature of the cell, in this case 433 K (160 °C) and RH is the relative humidity. The voltage loss for the ORR, where $p_{O_2} = 101.3$ kPa, is given by Eq. (3):

$$\eta_{ORR} = b \log\left[\frac{i + i_x}{10 L_{ca} A_{Pt,el} i^*_{o,s} \exp[-E_c^{rev}/RT(1 - T/T^*)]}\right] \quad (3)$$

where b is the Tafel slope, $2.303RT/\alpha_c F$ and α_c, taken to be one as in many publications [7,14–17], is the cathodic transfer coefficient (i.e. the product of the symmetry parameter, β, and the number of electrons transferred in the reaction (n)) [18], i_x the current due to H_2 gas crossover from the anode to the cathode, the factor 10 in the denominator is for unit conversion purposes, L_{ca} ($mg_{Pt}\,cm^{-2}$) the cathode Pt loading, $A_{Pt,el}$ (m^2_{Pt}/g^{-1}_{Pt}) the real Pt surface area in the MEA, $i^*_{o,s}$ the catalyst specific exchange current density normalized to reference oxygen partial pressure of 101.3 kPa and a reference temperature (T^*) of 333 K (60 °C), and E_c^{rev} is the activation energy of the ORR at the reversible cell potential (zero overpotential).

Conversely, one can arrive at the equivalent expected potential ($E_{iR\text{-free}}$) by correcting the observed cell voltage (E_{cell}), produced in the absence of mass transport and HOR overpotential losses, for membrane protonic and cell electronic resistances (R_Ω) as shown in Eq. (4):

$$E_{iR-free} = E_{cell} + iR_\Omega \quad (4)$$

Hence, the *predicted* cell voltage, using values of $i^*_{o,s}$ (obtained from MEA studies [19]) and E_c^{rev} (obtained from liquid electrolyte experiments [20]) for the ORR on Pt–Ni/C, along with Eqs. (1)–(3), and the observed ohmic-free cell voltage (obtained *experimentally* using Eq. (4)) should be equivalent, as presented in Eq. (5):

$$E_{rev} - \eta_{ORR} = E_{cell} + iR_\Omega \quad (5)$$

3. Experimental

3.1. Cell preparation and operating conditions

A phosphoric acid doped polybenzimidazole membrane, sandwiched by a 1.0 $mg_{pt}\,cm^{-2}$ Pt anode and 0.7 $mg_{pt}\,cm^{-2}$ Pt–Ni/C alloy cathode was used in this study and purchased commercially. The membrane had an in situ (compressed) thickness of 100 μm. The thicknesses of the anode and cathode layer (i.e. catalyst layer plus diffusion media) were 415 and 350 μm, respectively. Gasket thicknesses of 400 μm were used to compress the MEA between 12 and 15% at 50 inch/pounds of torque.

The single cell was conditioned at 160 °C and 0.2 A cm^{-2} for about 24 h. Neat H_2 and O_2 flows of 100 sccm with no additional humidification were used as reactant gases. The cell and gas pressures were kept at ambient pressure throughout the study (i.e. $p_{H_2} = p_{O_2} = 101.3$ kPa). After the conditioning period, a polarization curve (0.02, 0.03, 0.05, 0.1, 0.2, and 0.4 A cm^{-2}) was taken at 160 °C, with a Solartron SI 1287 electrochemical interface. Each current density was held for 20–25 min, though a steady voltage was observed within the first few.

3.2. ac impedance

A Solartron SI 1287 impedance/gain-phase analyzer was used to produce full frequency ac impedance spectra (100 kHz to 0.1 Hz) following each point on the polarization curve. The intercept with real axis, measuring zero imaginary impedance (zero phase angle), was taken to be the cell resistance (sum of the protonic membrane resistance and the cells electronic resistance).

3.3. Quantifying cell electronic resistance

A completely identical cell, less a membrane, was built to determine the sum of the experimental cell's electronic resistances, i.e. contact resistances between the flow fields and DMs as well as bulk electronic resistances of the DMs and microporous layers. The method was similar to previous studies by Neyerlin et al. [7,21,22].

3.4. Quantifying anode overpotential

A hydrogen pump or hydrogen concentration cell was set up in a similar fashion to that previous described [12,21,22]. This experiment, however, was conducted at 160 °C with a hydrogen flow of 100 sccm. Pressure drop between the anode and cathode side was minimal (<1 kPa) resulting in an open cell voltage of 0.6 mV.

3.5. Hydrogen crossover

Hydrogen permeability was determined in a method similar to that described by Inaba et al. [23]. Neat H_2 and N_2 were fed in with no additional humidification at ambient pressure with flow rates of 100 sccm to the anode and cathode, respectively. Voltage was swept from the equilibrated rest potential (about 120 mV) to 400 mV at 10 mV s^{-1}. The resulting current was due to hydrogen permeability through the membrane.

3.6. Electrochemical surface area

Hydrogen adsorption/desorption data was collected via cyclic voltammetry for the purpose of determining the cathode catalyst's real surface area. The cell was kept at 25 °C and ambient pressure while reactant gases with no additional humidification were passed through the cell. Hydrogen and nitrogen were supplied at a 25 sccm to the cathode and anode, respectively. Voltage

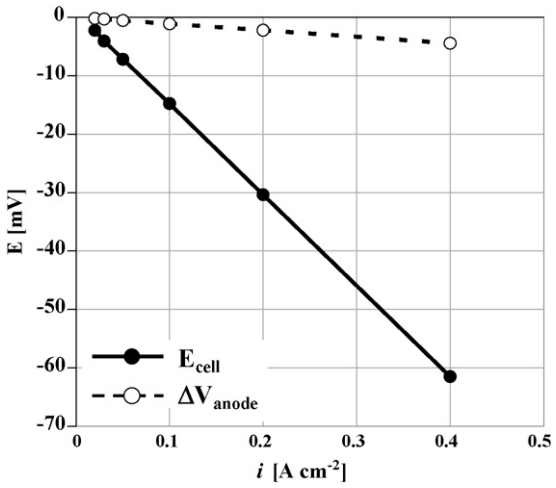

Fig. 1. Cell voltage (solid line) and anticipated anode voltage loss (dashed line) vs. current density for a hydrogen concentration cell with a H_3PO_4 doped PBI membrane having a 1.0 mg_{Pt} cm^{-2} anode and a 0.7 $mg_{Pt–Ni}$ cm^{-2} cathode, operating at 160 °C and dry hydrogen at ambient pressure.

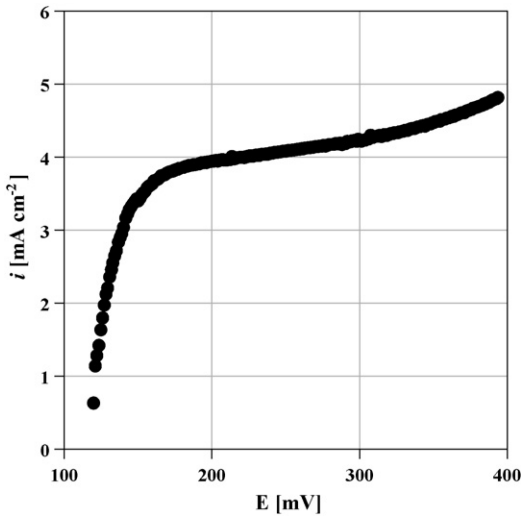

Fig. 2. Current due to hydrogen crossover as a function of current for a cell operating at 160 °C with dry H_2 and N_2 at ambient pressure.

was swept at a rate of 10 mV per second from 0.05 to 0.5 V and plotted versus the corresponding current. After correcting for crossover current, the electrochemical surface area was determined by integrating the H-adsorption charge in the cathodic sweep (shaded area in Fig. 3).

4. Results and discussion

4.1. Quantifying anode overpotential

A hydrogen pump or hydrogen concentration cell was used to confirm the assumption of negligible anode overpotential in a high temperature phosphoric acid doped PBI membrane. Fig. 1 displays the voltage of a hydrogen-pumping cell (solid symbols, solid line) and the anode voltage loss (hollow symbols, dashed line) versus current density at 160 °C and ambient pressure (i.e. $p_{H_2} \approx 101.3$). The anode voltage loss is calculated based on the measured cell voltage, R_Ω (measured after each point), and the ratio of anode catalyst layer thickness to total catalyst layer thicknesses (γ). In other words the ohmic losses and overpotential are assumed to be evenly distributed and we are trying to extract only those occurring on the anode side.

$$\Delta V_{\text{anode}} = \gamma(E_{\text{cell}} - iR_\Omega) \quad (6)$$

Fig. 1 illustrates that anode voltage loss is negligible, a mere 4–5 mV at 0.4 A cm^{-2}. Thus, any difference between the predicted and observed voltages more substantial than ~15 mV would represent a *significant* discrepancy.

4.2. Hydrogen crossover

To eliminate the possibility that hydrogen permeation through the membrane, and a corresponding crossover current, may compromise the conclusion of the study, a hydrogen crossover current was determined experimentally and accounted for in the experimental data. As seen in Fig. 2, the current was determined to reside between 4 and 5 mA cm^{-2} at 160 °C. A value of 4 mA cm^{-2} was accounted for when plotting the experimental current densities (i.e. plotted values for current density in Fig. 4 include the applied current plus the crossover current). These values correspond to a H_2 permeability between 2.0 and 2.5×10^{-15} mol cm cm^{-2} s^{-1} Pa^{-1}, which is in good agreement with the value of $1.2–4.0 \times 10^{-15}$ mol cm cm^{-2} s^{-1} Pa^{-1} reported for acid doped PBI at 160 °C by He et al. [24].

4.3. Catalyst surface area

In order to "personalize" the predicted voltage to this particular the test cell, a value for the real catalyst surface area, $A_{\text{Pt,el}}$ in Eq. (3), had to be established. Fig. 3 shows a CV for the cathode side of the MEA, a Pt–Ni/C catalyst with a loading

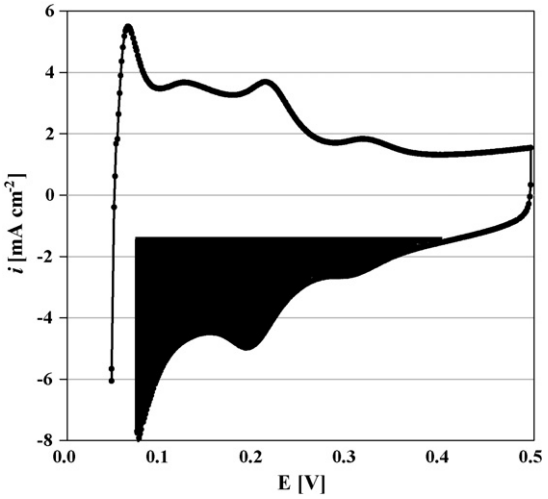

Fig. 3. CV of a 0.7 mg cm^{-2} Pt–Ni/C cathode at 25 °C with dry H_2 and N_2 at ambient pressure using a sweep rate of 10 mV s^{-1}. The real electrochemical surface area was obtained from integration of the H adsorption area (shaded region).

of 0.7 $mg_{pt}\,cm^{-2}$. The real Pt surface area was resolved from the hydrogen adsorption area (shaded portion) of Fig. 3, assuming that the charge came only from hydrogen interaction with the Pt surface [25], which has a corresponding surface charge of 210 $\mu C\,cm^{-2}{}_{Pt}$ [26]. The obtained ESA value of 38 $m^2\,g^{-1}{}_{Pt}$ was well within the expected range of 36–50 $m^2\,g^{-1}{}_{Pt}$ previously reported for Pt–Ni catalysts [25,27].

4.4. Membrane conductivity

While the method of comparison here utilizes ohmic-free voltages, the power output of a fuel cell is related to the actual cell voltage and the current density at which it is observed. The main difference between the two voltages, of course, results from proton conduction through the cell membrane. Thus, membrane conductivity is a vital diagnostic when it comes to cell performance. Fig. 4a shows full frequency sweep ac impedance data, collected after each data point on the polarization curve. Fig. 4b shows a zoom-in of the high frequency intercept with the real axis, zero imaginary resistance, which was used to obtain values for membrane protonic plus cell electronic resistances (R_Ω). To attain values for membrane conductivity, the cells electronic resistance (R_{e-}), measured to be 0.055 $\Omega\,cm^2$ (see Section 3), was subtracted from R_Ω and divided into the membranes thickness ($\delta_{mem} \approx 100\,\mu m$) as described by Eq. (7):

$$\kappa_{mem} = \frac{\delta_{mem}}{R_\Omega - R_{e-}} \tag{7}$$

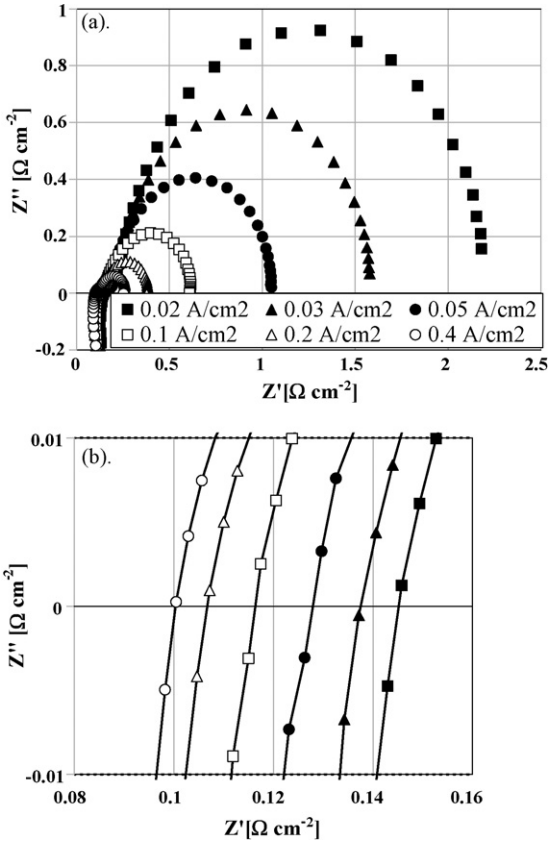

Fig. 4. (a) Full frequency ac impedance sweeps taken after 20–25 min equilibration periods for a cell operating at 160 °C with dry H_2 and O_2 at ambient pressure for various current densities. (b) Zoom-in of the high frequency, real intercept region of (a).

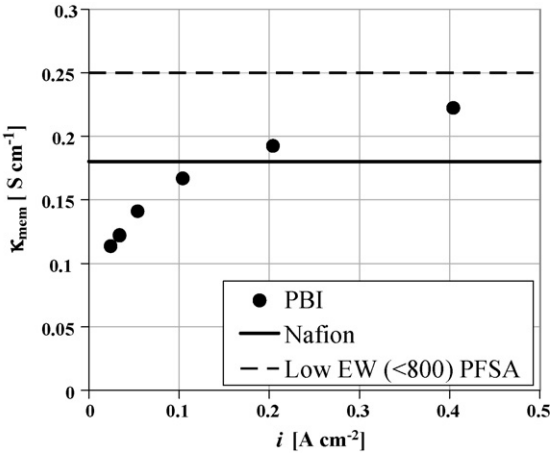

Fig. 5. Proton conductivity vs. current density for a PBI-based material (solid circles) at 160 °C with no external humidification. Also displayed are the proton conductivities for Nafion® 112 (solid line) and a Low EW PFSA (dashed line) at 100% RH and 80 °C.

The resulting values for membrane conductivity as a function of current are displayed in Fig. 5 (solid circles). For comparison, these values are plotted along with conductivity values for two other membranes. Both the values for Nafion® (solid line) and low EW (<800) PFSA (dashed line)) membrane conductivity were obtained at 80 °C and 100% RH [28] and, for simplicity, assumed to be constant with increasing current density. It is evident from this comparison that the PBI-based membrane falls short of Nafion® conductivity at low current densities (<0.2 $A\,cm^{-2}$) but overtakes it at high current densities, most likely from the benefit of increased water production. Consequently, the PBI-based material can be considered a viable solution for high temperature and zero RH fuel cell performance; at least as far as membrane conductivity is concerned.

4.5. Predicted performance

Previous results for oxygen reduction on Pt–Ni/C catalysts were used to formulate a kinetic performance baseline for MEA operation at 160 °C and 1% RH (note the thermodynamic effects of the water vapor pressure are accounted for in Eq. (2)). An exchange current density for the ORR on Pt–Ni/C at 80 °C and $p_{O_2} = 101.3$ kPa ($i^*_{o,s} = 3.3 \times 10^{-8}\,A\,cm^{-2}{}_{Pt}$) was extracted from data taken on MEA's (with a Nafion® like ionomer) by Wagner's group [19], while an activation energy at zero overpotential ($E_c^{rev} = 51\,kJ\,mol^{-1}$) was determined from the data of Stamenkovic et al. [20]. These values were then used, along with the value previously determined for real Pt surface area ($A_{Pt,el} = 38.4\,m^2\,g^{-1}{}_{Pt}$) and Eqs. (1)–(3), to establish the predicted performance for a phosphoric acid doped PBI membrane having a 0.7 $mg_{Pt}\,cm^{-2}$ Pt–Ni/C cathode (solid line Fig. 6a). For comparison later, the predicted performance for an

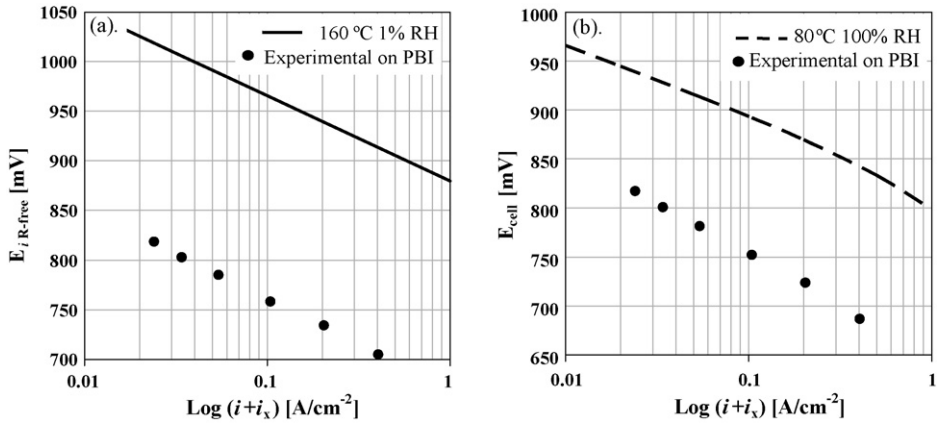

Fig. 6. (a) *iR*-free voltage vs. current density for the tested MEA based on a PBI material (solid circles) and calculated for a Pt–Ni/C catalyst with an $i^*_{o,s} = 3.3 \times 10^{-8}$ A cm$^{-2}{}_{Pt}$ at 160 °C and 1% RH (dashed line). (b) Observable cell voltage for the tested MEA based on a PBI material (solid circles) and calculated for a Pt–Ni/C catalyst with a $i^*_{o,s} = 3.3 \times 10^{-8}$ A cm$^{-2}{}_{Pt}$ at 80 °C and 100% RH (dashed line).

MEA operating at 80 °C and 100% RH, with all other parameters unchanged, is plotted in Fig. 6b (dashed line Fig. 6b).

4.6. Experimental test results

The circular data points in Fig. 6a represents the observed experimental cell voltage corrected for both hydrogen gas crossover as well as membrane protonic and cell electronic resistances (R_Ω) (see Eq. (4)). In theory the experimental values should lie on top of the solid line predicted for a Pt–Ni/C catalyst at 160 °C and 1% RH. While the theorized performance and the observed performance have similar Tafel slopes (86 and 91 mV dec^{-1}, respectively) they are offset by about 200 mV across the range of currents examined, which equates to about a two orders of magnitude difference in the exchange current density (a decrease from 8.2×10^{-7} to 4–5 $\times 10^{-9}$ A cm$^{-2}{}_{Pt}$). The value of $i_{o,s}$ attained here (4–5 $\times 10^{-9}$ A cm$^{-2}{}_{Pt}$) for the ORR on Pt–Ni/C at 160 °C, with a H_3PO_4 doped PBI membrane having zero added humidification, is close to the value of $2.2 \pm 1.2 \times 10^{-9}$ A cm$^{-2}{}_{Pt}$ reported by Liu et al. for oxygen reduction on a Pt/C catalyst at 150 °C, having a H_3PO_4 doped PBI membrane with 1% RH [29].

Recalling that the exchange current used for performance prediction was determined from data taken at 100% RH, it has been previously proposed that, for both electrodes which use Nafion® like ionomers [21] as well as for H_3PO_4 PBI-based MEAs [29], at low RH the reduction in proton concentration or availability results in a decrease in $i_{o,s}$ for the ORR. Though some reduction in $i_{o,s}$ is anticipated in light of this effect, the extent to which $i_{o,s}$ is reduced here greatly exceeds literature predictions; Neyerlin et al. reported only a two fold reduction in $i_{o,s}$ as RH was lowered from 100 to 30% [21], while Liu et al. reported a similar reduction while lowering RH from 15 to 1% [29]. Furthermore, since the conductivity of the PBI-based membrane in this study is similar to that of Nafion® at 100% RH, it would be difficult to envision that a reduced proton concentration/activity was the cause of the reduction in kinetics, despite the fact that no additional humidification was provided in this study (i.e. the activity of protons should be similar in the two materials).

The bulk of the reduced performance for the ORR on a Pt-based catalyst is likely due to the adsorption effects of the $H_2PO_4^-$ as has been previously proposed [10,11,30–33]. Significant reduction of ORR kinetics (25–200 mV) on Pt/C in the presence of anions, be it Cl^- [34], Br^- [35], or $H_2PO_4^-$ [31,32], has been shown to occur even at modest anion concentrations (0.1–0.38 mM). Though many studies have been done regarding anion adsorption, few have attempted to quantify the extent to which the exchange current density of the ORR was decreased in an MEA, as done here. With so much focus on high temperature operation, for the reasons discussed in the introduction, it is important to view performance relative to the maximum possible performance at a given condition, as well as to compare experimental results with other technological possibilities.

The dashed line in Fig. 6b represents the predicted observable cell voltage for PEMFC operation at 80 °C and 100% RH, utilizing a Nafion® 112 membrane. The voltages plotted in Fig. 6b are *iR*-free voltages less the resistance from membrane proton conduction only (does not include any contact or bulk electronic resistances). The purpose of this comparison is to highlight the difference in the utilization of resources for the two technologies. While the PBI-based MEA does provide for high temperature operation and reasonable conductivity, the kinetic benefits of such high temperature operation on the ORR are completely lost due to the adsorption of $H_2PO_4^-$. What's more, current Nafion® 112 MEAs operating at 80 °C and 100% RH out perform the PBI-based technology by as much as 150 mV at 0.4 A cm^{-2}, equating to 25% more power output at said current density.

Keeping in mind that the purpose of the PBI-based MEA is only to allow for high temperature operation, further studies are planned to examine the extent to which high temperature operation does indeed inhibit CO poising.

5. Conclusions

The performance of a phosphoric acid doped PBI (polybenzimidazole) membrane, with Pt and Pt–Ni/C catalysts on the anode and cathode, respectively, was experimentally determined at 160 °C using neat H_2 and O_2. The resulting current voltage

relation was then compared to a performance curve calculated from previously established values for the exchange current density and activation energy of the oxygen reduction reaction (ORR) on Pt–Ni/C. An overall voltage loss >200 mV, regardless of current density, was observed for the MEA relative to the predicted performance, implying about two orders of magnitude decrease in the exchange current density for the ORR. The reduction in $i_{o,s}$ was attributed to the adsorption of anions, specifically $H_2PO_4^-$, as has been previously postulated [10,11,30–33].

Acknowledgements

The authors want to thank the U.S. Dept of Army and Army Material Command for financial support.

References

[1] D.A. Masten, A.D. Bosco, in: W. Vielstich, A. Lamm, H.A. Gasteiger (Eds.), Handbook of Fuel Cells: Fundamentals, Technology, and Applications, 4, Wiley, 2003, p. 714, Chapter 53.
[2] M.F. Mathias, H.A. Gasteiger, Proceedings of the Proton Conducting Membrane Fuel Cells III Symposium, Salt Lake City, UT, Fall, 2002.
[3] G. Ertl, M. Neumann, K.M. Streit, Surf. Sci. 64 (1977) 393.
[4] Y.Y. Yeo, L. Vattuone, D.A. King, J. Chem. Phys. 106 (1997) 392.
[5] S. Westerberg, C. Wang, G.A. Somorjai, Surf. Sci. 582 (2005) 137–144.
[6] S. Gottesfeld, J. Pafford, J. Electrochem. Soc. 135 (1988) 2651.
[7] K.C. Neyerlin, W. Gu, J. Jorne, H.A. Gasteiger, J. Electrochem. Soc. 153 (2006) A1955–A1963.
[8] R.F. Savinell, E.B. Yeager, J. Electrochem. Soc. 141 (1994) L46.
[9] R.F. Savinell, M.H. Litt, U.S. Patent 5,525,436 (1996).
[10] J. Lobato, P. Canizares, M.A. Rodrigo, J. Linares, Electrochim. Acta 52 (2007) 3910–3920.
[11] Q. Li, R. He, J.O. Jensen, N.J. Bjerrum, Fuel Cells 4 (2004) 147–159.
[12] K.C. Neyerlin, W. Gu, J. Jorne, H.A. Gasteiger, J. Electrochem. Soc. 154 (2007) B631–B635.
[13] D.M. Bernardi, M.W. Verbugge, J. Electrochem. Soc. 139 (1992) 2477.
[14] S. Mukerjee, S. Srinivasan, A.J. Appleby, J. Electrochim. Acta 38 (1993) 1661.
[15] D. Thompsett, in: W. Vielstich, A. Lamm, H.A. Gasteiger (Eds.), Handbook of Fuel Cells: Fundamentals, Technology, and Applications, 3, Wiley, 2003, p. 538, Chapter 43.
[16] H.A. Gasteiger, W. Gu, R. Makharia, M.F. Mathias, B. Sompalli, in: W. Vielstich, A. Lamm, H.A. Gasteiger (Eds.), Handbook of Fuel Cells: Fundamentals, Technology, and Applications, 3, Wiley, 2003, p. 593, Chapter 46.
[17] X. Wang, I.-M. Hsing, P.L. Yue, J. Power Sources 96 (2001) 282–287.
[18] A.J. Bard, L.R. Faulkner, Electrochemical Methods, Wiley and Sons Inc., New York, 1980.
[19] Wagner F.T., Personal Commun., July 2007.
[20] V. Stamenkovic, T.J. Schmidt, P.N. Ross, N.M. Markovic, J. Electroanal. Chem. 554–555 (2003) 191–199.
[21] K.C. Neyerlin, H.A. Gasteiger, C.K. Mittelsteadt, J. Jorne, W. Gu, J. Electrochem. Soc. 152 (2005) A1073–A1080.
[22] K.C. Neyerlin, W. Gu, J. Jorne, J.A. Clark, H.A. Gasteiger, J. Electrochem. Soc. 154 (2007) B279–B287.
[23] M. Inaba, T. Kinumoto, M. Kiriake, R. Umebayashi, A. Tasaka, Z. Ogumi, Electrochim. Acta 51 (2006) 5746–5753.
[24] R. He, Q. Li, A. Bach, J.O. Jensen, N.J. Bjerrum, J. Membr. Sci. 277 (2006) 38–45.
[25] U.A. Paulus, A. Wokaun, G.G. Scherer, T.J. Schmidt, V. Stamenkovic, N.M. Markovic, P.N. Ross, Electrochim. Acta 47 (2002) 3787–3798.
[26] F.C. Nart, W. Vielstich, in: W. Vielstich, A. Lamm, H.A. Gasteiger (Eds.), Handbook of Fuel Cells: Fundamentals, Technology, and Applications, 2, Wiley, 2003, p. 302, Chapter 21.
[27] H. Yang, C. Coutanceau, J.M. Leger, N. Alonso-Vante, C. Lamy, J. Electroanal. Chem. 576 (2005) 305–313.
[28] M.F. Mathias, R. Makharia, H.A. Gasteiger, J.J. Conley, T.J. Fuller, C.J. Gittleman, S.S. Kocha, D.P. Miller, C.K. Mittelsteadt, T. Xie, S.G. Yan, P.T. Yu, Electrochem. Soc. Interf. (2005) 24–35.
[29] Z. Liu, J.S. Wainright, M.H. Litt, R.F. Savinell, Electrochim. Acta 51 (2006) 3914–3923.
[30] K.-L. Hsueh, E.R. Gonzalez, S. Srinivasan, Electrochim. Acta 28 (1983) 691–697.
[31] P.N. Ross, P.C. Andricacos, J. Electroanal. Chem. 154 (1983) 205–215.
[32] J.B. Floriano, E.A. Ticianelli, E.R. Gonzalez, J. Electroanal. Chem. 367 (1994) 157–164.
[33] D.R. DeSena, E.R. Gonzalez, E.A. Ticianelli, Electrochim. Acta 37 (1992) 1855–1858.
[34] T.J. Schmidt, U.A. Paulus, H.A. Gasteiger, R.J. Behm, J. Electroanal. Chem. 508 (2001) 41–47.
[35] N.M. Markovic, H.A. Gasteiger, B.N. Grgur, P.N. Ross, J. Electroanal. Chem. 467 (1999) 157–163.